JOURNAL OF SOLID STATE CHEMISTRY 87, 186–194 (1990)

# Study of the Bipyramidal Site in Magnetoplumbite-like Compounds, $SrM_{12}O_{19}$ ($M$ = Al, Fe, Ga)

K. KIMURA, M. OHGAKI, K. TANAKA, H. MORIKAWA, AND F. MARUMO

*Research Laboratory of Engineering Materials, Tokyo Institute of Technology, Nagatsuta 4259, Midori, Yokohama 227, Japan*

Received September 6, 1989; in revised form March 26, 1990

Structures of magnetoplumbite-type crystals $SrM_{12}O_{19}$ ($M$ = Al, Fe, Ga) have been refined by the single-crystal X-ray diffraction method. The space group is $P6_3/mmc$ with $Z = 2$. The cell dimensions are $a = 5.5666(2)$ and $c = 22.0018(8)$ Å for $SrAl_{12}O_{19}$, $a = 5.8836(1)$ and $c = 23.0376(9)$Å for $SrFe_{12}O_{19}$, and $a = 5.7929(1)$ and $c = 22.8123(7)$ Å for $SrGa_{12}O_{19}$ at 22°C. Four structural models were tested with respect to the states of $M$ atoms at trigonal bipyramidal sites: central atom and split atom models with and without anharmonic thermal vibrations. The simple split atom model gave lower $R_w$ values than the central atom model with anharmonic thermal vibrations for $SrAl_{12}O_{19}$ and $SrGa_{12}O_{19}$, whereas it gave an $R_w$ value approximately equal to that given by the central atom model with anharmonic vibration for $SrFe_{12}O_{19}$. The present study suggested that the potential around the $M$ atom with trigonal bipyramidal coordination has double minima in all the magnetoplumbite-type crystals at lower temperatures. 

## Introduction

The crystal structure of magnetoplumbite $PbFe_{12}O_{19}$ was studied by Adelsköld (*1*), who revealed that it belongs to the hexagonal space group $P6_3/mmc$. In this structure Fe atoms are distributed over three crystallographically independent octahedral sites, one tetrahedral site, and one trigonal bipyramidal site. Further structure refinements on magnetoplumbite-type compounds (*2–8*) showed that an ambiguity remained about the exact location of the cation at the trigonal bipyramidal site. Namely, there are two probable models: in one model a five-coordinated cation locates at the 2*b* site on the mirror plane of trigonal bipyramid (central atom model), and in the other two half-cations locate at two equivalent 4*e* sites displaced from the mirror plane (split atom model). Recently structure refinement was carried out on $CaAl_{12}O_{19}$ (*9*) to clarify the exact location of the Al atom in the bipyramidal site, taking anharmonic thermal vibration of the Al atom into account.

This paper describes results of structure refinements on $SrM_{12}O_{19}$ ($M$ = Al, Ga, Fe) carried out to elucidate the precise structural features of the trigonal bipyramidal coordinations in this type of crystal.

## Experimental

*Preparation of crystals.* In the $SrO–Ga_2O_3$ system, $SrGa_{12}O_{19}$ crystals incongruently melt into $Ga_2O_3$ and a liquid at

0022-4596/90 $3.00

1550°C, and $SrGa_4O_7$ crystals incongruently melt into $SrGa_{12}O_{19}$ and a liquid at 1490°C (*10*). Therefore, $SrGa_{12}O_{19}$ crystals were synthesized by the following procedure. Reagent-grade $SrCO_3$ and $Ga_2O_3$ were wet-mixed to give the composition of $SrO \cdot 5.2Ga_2O_3$. The mixture was heated in a Pt crucible with a Keramax (lanthanum chromate) furnace up to 1500°C, kept at this temperature for 1 day, cooled to 1200°C with a cooling rate of 3°C/hr, kept at 1200°C for 1 day, again cooled to 1000°C with a cooling rate of 3°C/hr, and then quenched to room temperature.

The phase diagram of the system $SrO$–$Al_2O_3$ was reported by Massazza (*11*). However, details have not been yet established in the compositional range near $SrAl_{12}O_{19}$, since the melting point is rather high. Therefore, $SrAl_{12}O_{19}$ crystals were synthesized by solid-state reaction. Reagent-grade $SrCo_3$ and $Al_2O_3$ were wet-mixed to give the composition of $SrAl_{12}O_{19}$, and the mixture was put into an alumina crucible and calcined at 1400°C for 1 day in the Keramax furnace. The product was powdered and pressed into a pellet. The pellet was put into an alumina crucible and heated in the Keramax furnace to 1850°C, kept at 1850°C for 1 day, cooled to 1100°C with a cooling rate of 10°C/hr, and then quenched to room temperature.

Crystals of $SrFe_{12}O_{19}$ were synthesized by the flux method after Gambino and Leonhard (*12*), utilizing $Na_2O$ as the flux. Reagent-grade $SrCO_3$, $Fe_2O_3$, and $Na_2CO_3$ were wet-mixed to give the molar ratios of 15 : 62 : 23. The mixture was sealed in a Pt tube and heated to 1250°C in a Siliconit (SiC) furnace, kept at 1250°C for 1 day, cooled to 1000°C with a cooling rate of 3°C/hr, and then quenched to room temperature. The Sr $Fe_{12}O_{19}$ crystals were separated by using 20 mol% $HNO_3$ solution. To check dissolution of Na into the crystals, chemical analysis was carried out with an analytical electron microscope. Since the Na$K\alpha$ peak was not detected, the crystals were considered to be free from Na.

TABLE I

CRYSTAL DATA AT 22°C

| | $SrAl_{12}O_{19}$ | $SrGa_{12}O_{19}$ | $SrFe_{12}O_{19}$ |
|---|---|---|---|
| Space group | $P6_3/mmc$ | $P6_3/mmc$ | $P6_3/mmc$ |
| $Z$ | 2 | 2 | 2 |
| Cell dimensions | | | |
| $a$(Å) | 5.5666(2) | 5.7929(1) | 5.8836(1) |
| $c$(Å) | 22.0018(8) | 22.8123(7) | 23.0376(9) |
| $D_x$(g/cm$^3$) | 4.03 | 6.16 | 5.11 |
| $\mu$ for Mo$K\alpha$(cm$^{-1}$) | 58.4 | 295.0 | 165.7 |

*Intensity collection.* The space group was confirmed to be $P6_3/mmc$ with Weissenberg photographs on all the crystals. The cell dimensions were determined by the least-squares procedure from $2\theta$ values of reflections obtained on a four-circle diffractometer (Rigaku AFC-5UD) in the range $70° \leqq 2\theta \leqq 80°$, where peaks of $K\alpha_1$ and $K\alpha_2$ are separately recorded. The obtained values are given in Table I. The numbers of $2\theta$ values used for this purpose were 34, 96, and 107 in $SrAl_{12}O_{19}$, $SrFe_{12}O_{19}$, and Sr $Ga_{12}O_{19}$, respectively.

Hexagonal, platy crystals were used in all the intensity measurements. The sizes of the specimens are shown in Table II together with other experimental conditions. Intensities were measured on the four-circle diffractometer with Mo$K\alpha$ radiation ($\lambda$ = 0.71069 Å) monochromated with pyrolytic graphite at 22°C. Strong reflections in the lower angle range were measured in the full reciprocal space for corrections of anisotropic extinctions. The reflections satisfying the condition $|F_0| \geqq 3\sigma(|F_0|)$ were used in the subsequent calculations. The observed intensities were corrected for Lorentz polarization and absorption factors. Absorption corrections were carried out by taking the crystal shapes into consideration. The numbers of reflections used are 1449, 1883, and 2257 in $SrAl_{12}O_{19}$, $SrFe_{12}O_{19}$, and $SrGa_{12}O_{19}$, respectively, among which 189, 102, and 222 are

TABLE II
EXPERIMENTAL CONDITIONS

| | $SrAl_{12}O_{19}$ | $SrGa_{12}O_{19}$ | $SrFe_{12}O_{19}$ |
|---|---|---|---|
| Crystal shape | Hexagonal plate | Hexagonal plate | Hexagonal plate |
| Crystal size (mm) | | | |
| Edge length | 0.06 | 0.08 | 0.08 |
| Thickness | 0.04 | 0.06 | 0.04 |
| X-ray source | Mo$K\alpha$ | Mo$K\alpha$ | Mo$K\alpha$ |
| Monochromator | Graphite | Graphite | Graphite |
| $2\theta$ maximum (°) | 120 | 150 | 120 |
| Range of $h$, $k$, $l$ | $0 \leqq h, k \leqq 13$<br>$0 \leqq l \leqq 53$ | $0 \leqq h, k \leqq 15$<br>$0 \leqq l \leqq 62$ | $0 \leqq h, k \leqq 14$<br>$0 \leqq l \leqq 56$ |
| Scan mode | | | |
| $2\theta < 60°$ | $\omega$ scan | $\omega$ scan | $\omega$ scan |
| $60° \leqq 2\theta$ | $\omega - 2\theta$ scan | $\omega - 2\theta$ scan | $\omega - 2\theta$ scan |
| Scan width (°) | $1.0 + 0.5 \tan\theta$ | $1.0 + 0.5 \tan\theta$ | $1.3 + 0.5 \tan\theta$ |
| Scan speed in $\theta$ ($min^{-1}$) | 2° | 2° | 2° |
| Maximum repetition of scans | 3 | 3 | 3 |
| No. of measured reflections | 4436 | 5594 | 4213 |
| No. of observed reflections | 2553 | 3877 | 2774 |
| No. of reflections with $\lvert F_0\rvert \geqq 3\sigma(\lvert F_0\rvert)$ | 1449 | 2257 | 1883 |
| No. of independent reflections | 540 | 1121 | 944 |
| No. of reflections used for anisotropic extinction correction | 189 | 222 | 102 |

those measured for determination of anisotropic extinction parameters.

## Structure Refinement

Atomic scattering factors for $Al^{3+}$, $Fe^{3+}$, $Ga^{3+}$, and $Sr^{2+}$ ions and dispersion correction factors were taken from "International Tables for X-ray Crystallography" (*13*). The scattering factor given by Tokonami (*14*) was used for $O^{2-}$ ions. The structures were refined with a modified version of the full-matrix least-squares program LINKT85, which has functions for extinction correction after Becker and Coppens (*15*) and for anharmonic thermal parameter refinement with the procedure by Tanaka and Marumo (*16*). The refinements were carried out on the central atom and split atom models with respect to the cations at the trigonal bipyramidal sites, starting from the atomic parameters given for $CaAl_{12}O_{19}$ by Utsunomiya *et al.* (*9*). Unit weights were given to all the reflections.

First, refinements were carried out on the central atom model. The least-squares calculations assuming an anisotropic extinction effect of type II (*15*) with a Gaussian distribution gave reasonably small $R$ and $R_w$ values in $SrAl_{12}O_{19}$ and $SrGa_{12}O_{19}$, while those assuming an anisotropic extinction effect of type I diverged. Therefore, further refinements were continued on the assumption of the type II extinction effect on these crystals. On the other hand, the situation was reversed in $SrFe_{12}O_{19}$, and the refinements were performed by applying the type I extinction corrections. The final $R$ and $R_w$ values are given in Table III.

Next, the refinements were carried out on the split atom model. The least-squares calculations on this model gave $R$ and $R_w$ values a little lower than those in $SrAl_{12}O_{19}$ and $SrGa_{12}O_{19}$, whereas the final $R$ and $R_w$

TABLE III

$R$, $U_{11}$(Å$^2$), AND $U_{33}$(Å$^2$) VALUES OF $M$(2) ATOMS AND PEAK HEIGHTS ($e$/A$^3$) AROUND $M$(2) ATOMS ON THE DIFFERENCE FOURIER MAPS OBTAINED BY VARIOUS MODELS

| | $SrAl_{12}O_{19}$ | $SrGa_{12}O_{19}$ | $SrFe_{12}O_{19}$ |
|---|---|---|---|
| Central atom model | | | |
| $R$ | 0.0340 | 0.0347 | 0.0286 |
| $R_w$ | 0.0364 | 0.0364 | 0.0266 |
| $U_{11}$ | 0.0017 | 0.0028 | 0.0033 |
| $U_{33}$ | 0.0695 | 0.0493 | 0.0281 |
| Height of the positive peaks near $M$(2) | 1.1 | 4.3 | 0.6 |
| The site of the peak | 0, 0, 0.27 | 0, 0, 0.260 | 0, 0, 0.26 |
| Split atom model | | | |
| $R$ | 0.0331 | 0.0324 | 0.0285 |
| $R_w$ | 0.0353 | 0.0352 | 0.0265 |
| $U_{11}$ | 0.0024 | 0.0031 | 0.0034 |
| $U_{33}$ | 0.0094 | 0.0135 | 0.0130 |
| Height of the positive peaks near $M$(2) | 0.5 | 0.1 | 0[b] |
| The site of the peak | 0, 0, 0.27 | 0, 0, 0.265 | 0, 0, 0.26 |
| Central atom model[a] | | | |
| $R$ | 0.0331 | 0.0326 | 0.0284 |
| $R_w$ | 0.0354 | 0.0353 | 0.0264 |
| $U_{11}$ | 0.0020 | 0.0030 | 0.0036 |
| $U_{33}$ | 0.0255 | 0.0352 | 0.0261 |
| Height of the positive peaks near $M$(2) | 0.6 | 0.8 | 0.1[b] |
| The site of the peak | 0, 0, 0.27 | 0, 0, 0.265 | 0, 0, 0.26 |
| Split atom model[a] | | | |
| $R$ | 0.0331 | 0.0323 | 0.0284 |
| $R_w$ | 0.0353 | 0.0352 | 0.0264 |
| $U_{11}$ | 0.0024 | 0.0033 | 0.0035 |
| $U_{33}$ | 0.0104 | 0.0137 | 0.0130 |
| Height of the positive peaks near $M$(2) | 0.4 | 0.0 | 0.1[b] |
| The site of the peak | 0, 0, 0.27 | 0, 0, 0.260 | 0, 0, 0.26 |

[a] Anharmonic thermal vibration for $M$(2) atom.

[b] There is no peak around (0, 0, 0.26). The value is the residual density at (0, 0, 0.26).

values were virtually identical for the two models in $SrFe_{12}O_{19}$. The final atomic parameters of the split atom model are given in Table IV. Those of the central atom model are also given in the table for $SrFe_{12}O_{19}$.

The refinement on $SrGa_{12}O_{19}$ with the central atom model gave a $U_{33}$ value of 0.0493 Å$^2$ for the Ga(2) atom, which is extremely large compared with other thermal parameters. The difference Fourier map of this model showed a negative peak with a depth of $-3.7$ $e$/Å$^3$ at the Ga(2) site and two positive peaks with heights of 4.3 $e$/Å$^3$ at 0.2 Å apart from the Ga(2) site along the $c$ axis. On the other hand, the refinements allotting the Ga(2) atom at the 4$e$ sites statistically

TABLE IV

POSITIONAL AND THERMAL ($\times 10^4$) PARAMETERS FOR $SrM_{12}O_{19}$ ($M$ = Al, Ga, Fe)

| Atom | Position | $x$ | $y$ | $z$ | $U_{11}$ | $U_{22}$ | $U_{33}$ | $U_{23}$ |
|---|---|---|---|---|---|---|---|---|
| Sr | $2d$ | $\frac{2}{3}$ | $\frac{1}{3}$ | $\frac{1}{4}$ | 57(2) | $U_{11}$ | 57(3) | 0 |
| Al(1) | $2a$ | 0 | 0 | 0 | 41(5) | $U_{11}$ | 24(8) | 0 |
| Al(2) | $4e$ | 0 | 0 | 0.2596(1) | 24(6) | $U_{11}$ | 94(20) | 0 |
| Al(3) | $4f$ | $\frac{1}{3}$ | $\frac{2}{3}$ | 0.02803(7) | 35(3) | $U_{11}$ | 39(5) | 0 |
| Al(4) | $4f$ | $\frac{1}{3}$ | $\frac{2}{3}$ | 0.19050(6) | 42(3) | $U_{11}$ | 37(5) | 0 |
| Al(5) | $12k$ | 0.1684(1) | 0.3368(2) | −0.10834(3) | 32(2) | 33(3) | 46(3) | −6(4) |
| O(1) | $4e$ | 0 | 0 | 0.1483(1) | 34(7) | $U_{11}$ | 20(12) | 0 |
| O(2) | $4f$ | $\frac{2}{3}$ | $\frac{1}{3}$ | 0.0544(2) | 42(7) | $U_{11}$ | 59(11) | 0 |
| O(3) | $6h$ | 0.1817(3) | 0.3634(7) | $\frac{1}{4}$ | 49(8) | 19(12) | 52(9) | 0 |
| O(4) | $12k$ | 0.1548(2) | 0.3096(5) | 0.05166(8) | 37(5) | 25(8) | 47(6) | −5(6) |
| O(5) | $12k$ | 0.5022(3) | 1.0044(5) | 0.14809(1) | 40(5) | 41(7) | 63(7) | 14(7) |
| Sr | $2d$ | $\frac{2}{3}$ | $\frac{1}{3}$ | $\frac{1}{4}$ | 97(3) | $U_{11}$ | 85(3) | 0 |
| Ga(1) | $2a$ | 0 | 0 | 0 | 41(2) | $U_{11}$ | 40(3) | 0 |
| Ga(2) | $4e$ | 0 | 0 | 0.25724(8) | 31(2) | $U_{11}$ | 135(9) | 0 |
| Ga(3) | $4f$ | $\frac{1}{3}$ | $\frac{2}{3}$ | 0.02724(3) | 36(1) | $U_{11}$ | 47(2) | 0 |
| Ga(4) | $4f$ | $\frac{1}{3}$ | $\frac{2}{3}$ | 0.18993(3) | 42(1) | $U_{11}$ | 42(2) | 0 |
| Ga(5) | $12k$ | 0.16833(5) | 0.33666(10) | −0.10934(1) | 40(1) | 32(1) | 59(1) | 4(1) |
| O(1) | $4e$ | 0 | 0 | 0.1495(2) | 32(8) | $U_{11}$ | 63(13) | 0 |
| O(2) | $4f$ | $\frac{2}{3}$ | $\frac{1}{3}$ | 0.0553(2) | 41(8) | $U_{11}$ | 38(11) | 0 |
| O(3) | $6h$ | 0.1818(4) | 0.3636(8) | $\frac{1}{4}$ | 88(11) | 19(13) | 69(11) | 0 |
| O(4) | $12k$ | 0.1555(3) | 0.3111(6) | 0.0525(1) | 50(6) | 28(9) | 67(7) | −8(6) |
| O(5) | $12k$ | 0.5045(4) | 1.0089(8) | 0.1500(1) | 46(5) | 71(9) | 71(7) | 11(9) |
| Sr | $2d$ | $\frac{2}{3}$ | $\frac{1}{3}$ | $\frac{1}{4}$ | 122(2) | $U_{11}$ | 96(3) | 0 |
| Fe(1) | $2a$ | 0 | 0 | 0 | 49(2) | $U_{11}$ | 44(3) | 0 |
| Fe(2) | $4e^a$ | 0 | 0 | 0.2549(2) | 34(2) | $U_{11}$ | 130(17) | 0 |
| | $2b^b$ | 0 | 0 | $\frac{1}{4}$ | 36(2) | | 261(12) | |
| Fe(3) | $4f$ | $\frac{1}{3}$ | $\frac{2}{3}$ | 0.02718(2) | 40(1) | $U_{11}$ | 51(2) | 0 |
| Fe(4) | $4f$ | $\frac{1}{3}$ | $\frac{2}{3}$ | 0.19091(2) | 49(1) | $U_{11}$ | 50(2) | 0 |
| Fe(5) | $12k$ | 0.16886(4) | 0.33772(8) | −0.10917(1) | 46(1) | 37(1) | 65(1) | 4(1) |
| O(1) | $4e^a$ | 0 | 0 | 0.1514(2) | 48(6) | $U_{11}$ | 82(12) | 0 |
| | $4e^b$ | | | | 49(6) | | 81(12) | |
| O(2) | $4f^a$ | $\frac{2}{3}$ | $\frac{1}{3}$ | 0.0554(2) | 59(8) | $U_{11}$ | 69(11) | 0 |
| | $4f^b$ | | | 0.0553(2) | | | | |
| O(3) | $6h^a$ | 0.1819(2) | 0.3639(6) | $\frac{1}{4}$ | 124(8) | 60(10) | 68(8) | 0 |
| | $6h^b$ | | | | 126(8) | 59(10) | | |
| O(4) | $12k^a$ | 0.1564(2) | 0.3127(4) | 0.05252(7) | 49(4) | 40(6) | 66(5) | 10(5) |
| | $12k^b$ | | | | | 41(6) | | |
| O(5) | $12k^a$ | 0.5039(3) | 1.0078(5) | 0.15093(8) | 56(4) | 74(6) | 69(5) | 28(6) |
| | $12k^b$ | | | 0.15092(8) | 55(4) | | | 30(6) |

*Note.* The thermal parameters are of the form: $\exp[-2\pi^2(U_{11}h^2a^{*2} + U_{22}k^2b^{*2} + U_{33}l^2C^{*2} + 2U_{12}hka^*b^* + 2U_{23}klb^*c^* + 2U_{13}hla^*c^*)]$. $2U_{12} = U_{22}$; $2U_{13} = U_{23}$.

[a] Split atom model.

[b] Central atom model with anharmonic thermal vibration for Fe(2).

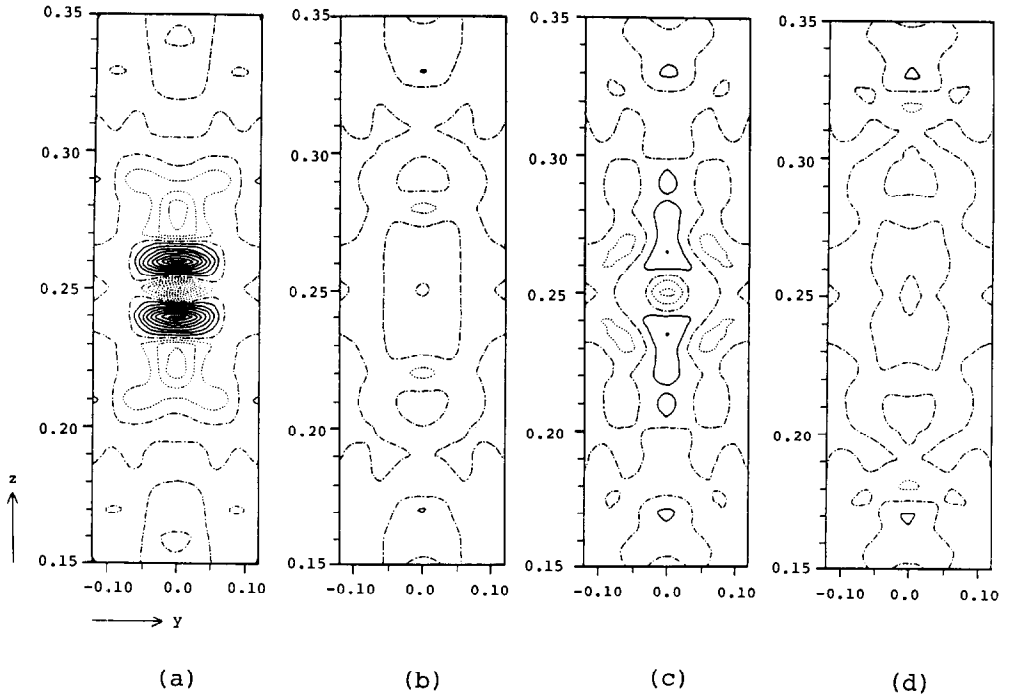


FIG. 1. Sections of the difference Fourier maps for $SrGa_{12}O_{19}$ with the plane $x = 0$ containing Ga(2) atoms at (0, 0, 0.25) after refinements with (a) the central atom model, (b) the split atom model, (c) the central atom model with anharmonic thermal vibration of the Ga(2) atom, and (d) the split atom model with anharmonic thermal vibration of the Ga(2) atom. Contours are at intervals of 0.5 $e/Å^3$. Positive, negative, and zero contours are in solid, broken, and dashed-dotted lines, respectively. O(1) atoms locate at (0, 0, 0.15) and (0, 0, 0.35).

(split atom model) reduced the $U_{33}$ value of the atom to 0.0135 $Å^2$, although the value was still larger than those of other atoms. The difference Fourier map gave quite small residual densities for this model. The negative peak at the Ga(2) site reduced the depth to 0.0 $e/Å^3$, and the two positive peaks reduced the heights to 0.1 $e/Å^3$ and shifted their centers to positions 0.4 Å apart from the Ga(2) site along the $c$ axis.

The larger $U_{33}$ value of Ga(2) and the residual densities around this atom may be ascribed to an anharmonic thermal vibration of the atom. Refinement was, therefore, carried out by introducing anharmonic terms to the thermal parameters of Ga(2) in the central atom model. The site symmetry of Ga(2) is $\bar{6}m2$ in this model, and anharmonic terms up to the fourth order were taken into account (*16*). The number of parameters increased is six compared with that of the harmonic model. The final $R$ and $R_w$ values were reduced to 0.033 and 0.035 with this refinement, respectively. The difference Fourier map showed a negative peak with a depth of $-1.3$ $e/Å^3$ at the Ga(2) site and two positive peaks with heights of 0.8 $e/Å^3$ at 0.2 Å apart from Ga(2) along the $c$ axis after this refinement.

The refinement of the split atom model with the anharmonic thermal parameters was further carried out. The site symmetry of Ga(2) is $3m$ in this model, and anharmonic terms up to the fourth order were

also taken into consideration. The number of parameters increased is nine compared with that of the harmonic model. The final $R$ and $R_w$ values were 0.0323 and 0.0352 in this refinement, respectively. The difference Fourier map showed a negative peak shallower than $-0.1$ $e/Å^3$ at the Ga(2) site and two positive peaks lower than 0.1 $e/Å^3$ at sites 0.2 Å from Ga(2) along the $c$ axis. The difference Fourier maps of $SrGa_{12}O_{19}$ after the respective refinements are compared in Fig. 1.

Similar refinements were carried out on $SrAl_{12}O_{19}$ and $SrFe_{12}O_{19}$ crystals. The Final $R$ and $R_w$ values, $U_{11}$ and $U_{33}$ of the $M(2)$ atoms with trigonal bipyramidal coordinations, and the heights of the peaks around the $M(2)$ sites in the difference Fourier maps are given in Table III together with those values of the harmonic models.

## Results and Discussion

In magnetoplumbite-type structures, $O^{2-}$ anions are arranged in a form of closest packing together with the larger cations ($Sr^{2+}$ in the present case), having the stacking sequence of |A B A B A C B C B C| A B A . . . along the $c$ axis. The $c$ period is completed by 10 layers, among which the third and eighth layers in the above sequence contain the larger cations as their constituents. There are 28 octahedral sites surrounded only by anions in a unit cell, 18 of which are occupied by $M^{3+}$ cations. Four $M^{3+}$ cations occupy tetrahedral sites and two $M^{3+}$ occupy the trigonal bipyramidal sites. The arrangement of the cations yields a spinel structure at the part where the stacking is the cubic closest one.

The interatomic distances calculated with the parameters listed in Table IV are given in Table V with their standard deviations. The effective ionic radius (*17*) decreases in the order $Fe^{3+}$, $Ga^{3+}$, and $Al^{3+}$, and correspondingly the size of the structure framework decreases in the same order. The average Sr–O distance also decreases in this order, having the values 2.884, 2.852, and 2.767 Å in $SrFe_{12}O_{19}$, $SrGa_{12}O_{19}$, and $SrAl_{12}O_{19}$, respectively.

TABLE V

INTERATOMIC DISTANCE (Å) IN $SrM_{12}O_{19}$ ($M$ = Al, Ga, Fe)

| | $SrAl_{12}O_{19}$ | $SrGa_{12}O_{19}$ | $SrFe_{12}O_{19}$ |
|---|---|---|---|
| $SrO_{12}$ polyhedron | | | |
| Sr–O(3) × 6 | 2.787(3) | 2.900(4) | 2.946(3) |
| Sr–O(5) × 6 | 2.746(2) | 2.803(3) | 2.821(2) |
| $M(1)O_6$ octahedron | | | |
| $M(1)$–O(4) × 6 | 1.876(2) | 1.967(7) | 2.001(2) |
| $M(2)O_5$ trigonal bipyramid | | | |
| $M(2)$–O(1) × 1 | 2.025(4) | 2.128(5) | 2.157(4) |
| $M(2)$–O(1)′ × 1 | 2.450(4) | 2.459(5) | 2.384(4) |
| Fe(2)–O(1)[a] × 2 | | | 2.272(4) |
| $M(2)$–O(3) × 3 | 1.765(3) | 1.831(4) | 1.858(3) |
| Fe(2)–O(3)[a] × 3 | | | 1.854(3) |
| $M(2)$–$M(2)'$ | 0.424(4) | 0.330(3) | 0.227(4) |
| O(3)–O(3)′[b] × 1 | 3.034(4) | 3.159(6) | 3.211(4) |
| $M(3)O_4$ tetrahedron | | | |
| $M(3)$–O(2) × 1 | 1.813(4) | 1.901(4) | 1.901(4) |
| $M(3)$–O(4) × 3 | 1.798(2) | 1.870(2) | 1.896(2) |
| $M(4)O_6$ octahedron | | | |
| $M(4)$–O(3) × 3 | 1.963(3) | 2.047(3) | 2.058(2) |
| $M(4)$–O(5) × 3 | 1.877(2) | 1.944(3) | 1.963(2) |
| $M(5)O_6$ octahedron | | | |
| $M(5)$–O(1) × 1 | 1.847(2) | 1.921(2) | 1.977(2) |
| $M(5)$–O(2) × 1 | 1.985(2) | 2.064(2) | 2.085(2) |
| $M(5)$–O(4) × 2 | 1.999(2) | 2.082(2) | 2.112(2) |
| $M(5)$–O(5) × 2 | 1.813(3) | 1.885(3) | 1.923(3) |

[a] Central atom model.
[b] O–O distance of the oxygen triangle on the mirror plane.

The $M(2)$–O bonds have longer average distances than those expected from the effective ionic radii (*17*). Namely, the observed values are 1.956, 2.018, and 2.023 Å for the split atom models of $SrAl_{12}O_{19}$, $SrGa_{12}O_{19}$, and $SrFe_{12}O_{19}$, respectively, whereas the sums of effective ionic radii are 1.88, 1.95, and 1.98 Å for fivefold coordinated $M^{3+}$ ions. Among the $M$–O distances listed in Table V, the $M(2)$–O(3) distances in the $M(2)O_5$ trigonal bipyramids are shortest and too short for the $M$–O distances even in the split atom model. The $M(2)$–O(3) distance becomes still shorter in the central atom model. This fact suggests that the central atom model is implausible.

The O(3)–O(3)′ edges of the trigonal bipyramids on the mirror planes have dis-

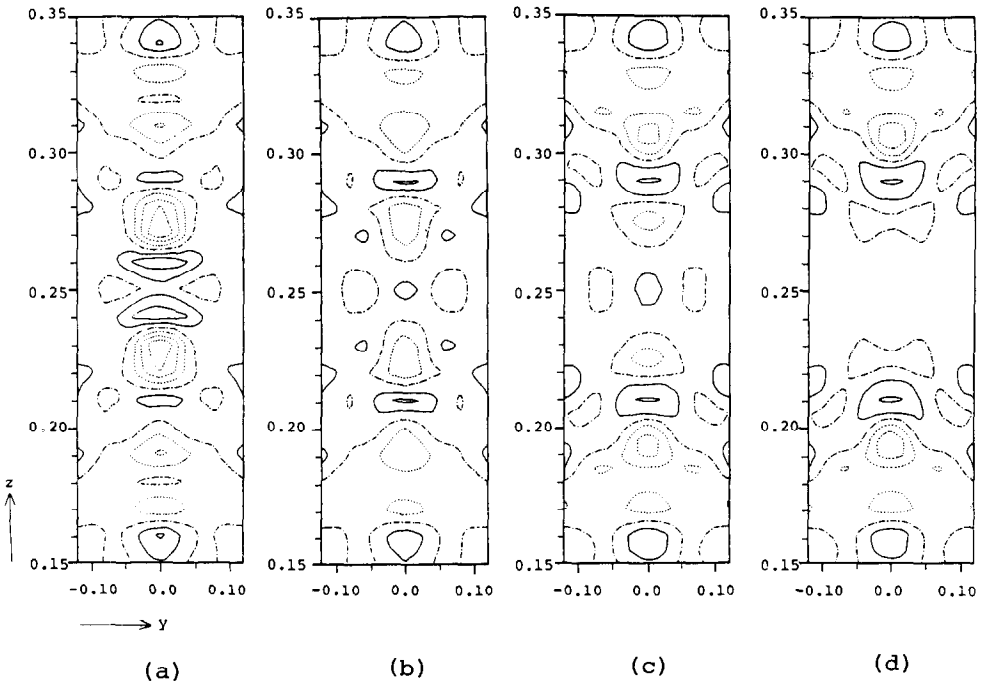


FIG. 2. Sections of the difference Fourier maps for $SrFe_{12}O_{19}$ with the plane $x = 0$ containing Fe(2) atoms at (0, 0, 0.25) after refinements with (a) the central atom model, (b) the split atom model, (c) the central atom model with anharmonic thermal vibration of the Fe(2) atom, and (d) the split atom model with anharmonic thermal vibration of the Fe(2) atom. Contours are at intervals of 0.2 $e/Å^3$. Positive, negative, and zero contours are in solid, broken, and dashed-dotted lines, respectively. O(1) atoms locate at (0, 0, 0.15) and (0, 0, 0.35).

tances 3.034, 3.159, and 3.211 Å in $SrAl_{12}O_{19}$, $SrGa_{12}O_{19}$, and $SrFe_{12}O_{19}$, respectively. This O(3)–O(3)′ separation acts as a potential barrier when the metal atom jumps between the two split atom sites. The Fe(2) atom in $SrFe_{12}O_{19}$ seems to jump most easily to the other site, since the O(3)–O(3)′ separation is the largest among the three compounds. The $M$(2)–$M$(2)′ separations are 0.227, 0.330, and 0.424 Å in the split atom models of $SrFe_{12}O_{19}$, $SrGa_{12}O_{19}$, and $SrAl_{12}O_{19}$, respectively. When the $M$(2)–$M$(2)′ separation decreases, the difference between the central atom and the split atom models becomes small. Actually the central atom model with anharmonic thermal vibration and the split atom model gave approximately equal $R_w$ values for $SrFe_{12}O_{19}$.

As seen in Table IV, the values of $U_{11}$ and $U_{33}$ for $M$ atoms range from 0.0024 to 0.0065 $Å^2$ in the split atom model except $U_{33}$ of the $M$(2) atom, which ranges from 0.0094 to 0.0135 $Å^2$. Namely the thermal ellipsoid of $M$(2) is extremely elongated along the $c$ axis. The $U_{11}$ and $U_{33}$ values of $M$(2) obtained in the four refinements are summarized in Table III. The refinements with the simple central atom model gave $U_{33}$ values ranging from 0.0281 to 0.0695 $Å^2$, which are much larger than those of other $M$ atoms. The values reduced to 0.0261–0.0352 $Å^2$ when the anharmonic thermal vibration was taken into consideration. On the other hand, the

refinements with the split atom model markedly reduced the $U_{33}$ values, although the values are still larger than those of other $M$ atoms.

The heights of residual densities in the difference Fourier maps around the $M(2)$ atoms are also given in Table III. The $M(2)$ atoms lie in deep negative regions after refinements with the central atom model, and pairs of high positive peaks exist on both sides of the atom along the $c$ axes in $SrAl_{12}O_{19}$ and $SrGa_{12}O_{19}$ (Fig. 1). The magnitudes of residual densities are significantly reduced after the refinement with the split atom model or the central atom model with allowance for anharmonic thermal vibration. However, the split atom model gives flatter difference Fourier maps than the central atom model with anharmonic thermal vibrations. Therefore, the split atom model seem to be most plausible among the three structure models in these two crystals.

On the other hand, the central atom model allowing anharmonic thermal vibration of the Fe(2) atom and the split atom model gave approximately equal $R_w$ values in the case of $SrFe_{12}O_{19}$. The residual densities are very small for both structure models as seen in Fig. 2. Thus, the present study cannot tell which model is closer to the real structural state in $SrFe_{12}O_{19}$. Mamalui *et al.* (*18*) reported from the evidence of the Mössbauer spectra of $BaFe_{12}O_{19}$ that the Fe atom at the bipyramidal site occupies one of two equivalent positions of the 4*e* sites statistically (the split atom model) at low temperature below 75 K and that it jumps between the two 4*e* sites at temperatures higher than 75 K. The result of the present study on $SrFe_{12}O_{19}$ accords well with this description.

The present study as well as Mössbauer measurements (*18, 19*) suggest that the potential around the $M(2)$ site has double minima in all the magnetoplumbite-type crystals at lower temperatures. Therefore, there are two plausible states for the $M(2)$ atoms at room temperature, that is to say, static disorder and dynamic disorder states. In the present study, introduction of anharmonic thermal vibration into the split atom model did not improve the $R_w$ value significantly and no definite conclusion was obtained on the states of $M(2)$ atoms. To settle this problem, analysis of diffuse scattering at various temperatures is required.

## References


1. V. Adelsköld, *Ark. Kemi Mineral. Geol. Ser. A* **12,** 1 (1938).
2. A. J. Lindop, C. Matthews, and D. W. Goodwin, *Acta Crystallogr. B* **31,** 2940 (1975).
3. M. Gasperin, M. C. Saine, A. Kahn, F. Laville, and A. M. Lejius, *J. Solid State Chem.* **54,** 61 (1984).
4. N. Iyi, Z. Inoue, S. Takekawa, and S. Kimura, *J. Solid State Chem.* **54,** 70 (1984).
5. N. Iyi, Z. Inoue, and S. Kimura, *J. Solid State Chem.* **54,** 123 (1984).
6. X. Obradors, A. Collomb, M. Pernet, D. Samaras, and J. C. Joubert, *J. Solid State Chem.* **56,** 171 (1985).
7. A. Kahn and J. Thery, *J. Solid State Chem.* **64,** 102 (1986).
8. X. Obradors, X. Solans, A. Collomb, D. Samaras, J. Rodriguez, M. Pernet, and M. Font-Altaba, *J. Solid State Chem.* **72,** 218 (1988).
9. A. Utsunomiya, K. Tanaka, H. Morikawa, F. Marumo, and H. Kojima, *J. Solid State Chem.* **75,** 197 (1988).
10. V. P. Kobzareva, L. M. Kovba, L. M. Lopato, L. N. Lykova, and A. V. Schevchenko, *Russ. J. Inorg. Chem. Engl. Transl.* **21,** 903 (1976).
11. F. Massazza, *Chem. Ind. (Milan)* **41,** 114 (1959).
12. R. J. Gambino and F. Leonhard, *J. Amer. Ceram. Soc.* **44,** 221 (1961).
13. "International Tables for X-ray Crystallography," Vol. IV, Kynoch Press, Birmingham (1974).
14. M. Tokonami, *Acta Crystallogr.* **19,** 486 (1965).
15. P. J. Becker and P. Coppens, *Acta Crystallogr. A* **31,** 417 (1975).
16. K. Tanaka and F. Marumo, *Acta Crystallogr. A* **39,** 631 (1983).
17. R. D. Shannon, *Acta Crystallogr. A* **32,** 751 (1976).
18. Y. A. Mamalui, U. P. Romanov, and K. M. Matsievskii, *Sov. Phys. Solid State Engl. Transl.* **21,** 117 (1979).
19. E. Kreber, V. Gonser, A. Trautwein, and F. Harris, *J. Phys. Chem. Solids* **36,** 263 (1975).